Environmental Technology
Publication details, including instructions for authors and subscription information:
http://www.tandfonline.com/loi/tent20

Oxidative decolorization of methylene blue by leached sea-nodule residues generated by the reduction-roasting ammoniacal leaching process

P. K. Satapathy [a] , N. S. Randhawa [b] & N. N. Das [a]

[a] P.G. Department of Chemistry, North Orissa University, Baripada, 757 003, Orissa, India

[b] Metal Extraction and Forming Division, National Metallurgical Laboratory, Jamshedpur, 831 007, India

Available online: 09 Jun 2011

To cite this article: P. K. Satapathy, N. S. Randhawa & N. N. Das (2011): Oxidative decolorization of methylene blue by leached sea-nodule residues generated by the reduction-roasting ammoniacal leaching process, Environmental Technology, DOI:10.1080/09593330.2011.584567

To link to this article: http://dx.doi.org/10.1080/09593330.2011.584567

Environmental Technology
iFirst, 2011, 1–8

Taylor & Francis
Taylor & Francis Group

Oxidative decolorization of methylene blue by leached sea-nodule residues generated by the reduction-roasting ammoniacal leaching process

P.K. Satapathy[a], N.S. Randhawa[b] and N.N. Das[a]*

[a]*P.G. Department of Chemistry, North Orissa University, Baripada – 757 003, Orissa, India;* [b]*Metal Extraction and Forming Division, National Metallurgical Laboratory, Jamshedpur – 831 007, India*

(*Received 22 October 2010; Accepted 26 April 2011*)

The leached residue, generated after selective extraction of Cu, Ni and Co by reductive-roasting ammoniacal leaching of sea nodules, was characterized by various physicochemical methods. The finely divided residue, containing mainly manganese carbonate/silicates and manganese(III,IV) (hydr)oxides along with iron oxides, showed a lower surface area (66.3 $m^2\ g^{-1}$) than that of the parent sea nodule (130 $m^2\ g^{-1}$). The catalytic efficiency of water-washed sea nodule residue (WSNR) was evaluated taking oxidative decolorization of methylene blue (MB) as the test reaction. The extent of decolorization was decreased with increase in pH but increased in the presence of H_2O_2 or NaCl. Decolorization of MB occurred in two consecutive steps; the rate constant of the first step was ∼10 times higher than that of the second step. The formation of a surface precursor complex between WSNR and MB at a rate-limiting step, followed by electron transfer from MB to the active metal centre of WSNR and release of product(s), was proposed as the decolorization process.

Keywords: dye; oxidative decolorization; methylene blue; sea nodules; leached residue

1. Introduction

Wastewaters generated from various industries like textile, paper, leather, food processing, cosmetics etc. contain residual dyes, which are not readily biodegradable. Because of their hazardous nature even at low concentrations, removal of these residual dyes has continued to be a major issue for discussion and regulation all over the world [1,2]. Several physical-, chemical/electrochemical- and biological-based processes are being used to treat these dyes containing effluents [3–8]. Among them, adsorption and chemical coagulation are two common techniques used most widely for treatment of these wastewaters, although they generate secondary wastes which require further treatment or disposal. In recent years extensive research has been dedicated to developing alternative processes for complete degradation of dyes to environmentally compatible products using suitable catalytic/photocatalytic systems. These include UV/H_2O_2, UV/O_3 or UV/Fenton's reagent, and TiO_2-based materials [9–13]. A number of manganese-based synthetic or naturally occurring materials have also been used for oxidative/photocatalytic degradation of a variety of dyes including methylene blue [14–19]. Methylene blue, a brightly coloured cationic thiazine dye used in textile industries, has several harmful effects on humans.

Sea nodules have been viewed as a reserve for strategic metals like Cu, Co and Ni (together constituting about 2.5 wt% of a manganese nodule) for future generation [20]. Several processes are now under trial across the globe to install commercial plants for extraction of these base metals economically [21–25]. The reductive ammoniacal leaching ($NH_4OH/(NH_4)_2SO_4$) and reduction-roast ammoniacal leaching ($NH_4OH/(NH_4)_2CO_3$) processes are under active consideration for setting up as commercial plants in the future [21–23]. Both the processes selectively leach out the base metals like Cu, Co and Ni along with Mn and Fe, leaving behind more than 70% residue as wastes for disposal. Owing to increasingly stringent disposal rules, it has become imperative to develop methods for proper utilization of such huge quantities of leached residues. These leached residues containing oxides/oxyhydroxides of Fe, Mn, Al and Si, with reasonable porosity and surface area, showed good adsorption capacity for several bivalent metal ions and oxyanions [26–28]. Moreover, Fe and Mn in these residues are present in variable oxidation states. In view of the above characteristics, one can envisage the use of leached residues as an effective oxidation catalyst for a variety of organic contaminants.

The present study aimed to explore the feasibility of sea-nodule leached residue as an oxidation catalyst for decolorization of dyes using a model cationic dye, methylene blue (MB). The effects of various parameters like initial dye concentration, catalyst dose, pH and salt on decolorization of MB were also studied and the results were compared with the activity of the parent sea nodule. Moreover, this

*Corresponding author. Email: dasnn64@rediffmail.com

ISSN 0959-3330 print/ISSN 1479-487X online

http://dx.doi.org/10.1080/09593330.2011.584567
http://www.tandfonline.com

is an attempt towards developing catalysts from wastes containing transition metal compounds [29].

2. Experimental

2.1. Materials

The sample of sea-nodule leached residue (SNR) used in the present study, generated from reduction roasting of sea nodules at 750 °C followed by ammoniacal leaching, was collected from the pilot plant operated at Hindustan Zinc Limited, Udaipur, India. The parent Indian Ocean sea nodule (SN), which generates the residue after the leaching process, was also collected for comparison of activity. The samples were air dried for several days, mixed thoroughly and kept in airtight bottles for characterization and further use. To remove the loosely associated metal ions/anions, the leached residue was washed with distilled water. In typical lots, 50 g of the leached residue was dispersed in 500 mL of distilled water (solid:liquid ratio 1:10) and stirred for 2 h at room temperature. The solid was separated by filtration, washed with distilled water, air dried for several days and used for further characterization as well as for decolorization experiments. The water-washed sea-nodule residue is designated as WSNR.

Stock solution (1.0 g L^{-1}) of MB (3,7-(dimethylamino)-phenazathionium chloride) was prepared from an AR-grade sample, and the working solutions were prepared by suitable dilution of the stock with distilled water. The pH of the dye solutions was adjusted to the desired values using dilute NaOH or HCl. All other chemicals used in this study were of extra-pure or analytical grades.

2.2. Characterization of materials

Chemical analyses for major and minor constituents in different samples were done as described earlier by conventional wet chemical methods and atomic absorption spectrometry AAS (Avanta, GBC), respectively [28]. Thermogravimetric/differential thermal analysis (TG-DTA) of SNR was carried out in static air using a Shimadzu DT 40 thermal analyser in the temperature range 30–1000 °C at a heating rate of 10 °C min^{-1} using α-Al_2O_3 as reference.

The particle size of SNR was determined using a Malvern SA-CP3 Particle Size Analyser. The X-ray diffraction (XRD) patterns were recorded on a Siemens D 500 X-ray diffractometer using CuK_α radiations. Fourier transform infrared (FT-IR) spectra in KBr pellets were collected using a ThermoNicolet 870 FT-IR in absorption mode averaging 32 scans and at a resolution of 4 cm^{-1}. Surface areas were determined by the BET method using a Nova 4000e (Quantachrome, USA). The point of zero charge (pH_{pzc}) of WSNR was determined by the batch acid-base titration method of Huang and Ostavic [30]. All pH measurements, including those of the adsorption studies, were done with a Toshniwal CL 54 digital pH meter using a combined glass electrode. The pH meter was standardized with NBS (US National Bureau of Standards) buffers before any pH measurement.

2.3. Oxidative decolorization of MB

The oxidative decolorization of MB was carried out by batch technique at constant temperature (25 ± 0.5 °C) and stirring speed in dark and static air. Based on some preliminary experiments, the different parameters affecting the decolorization were varied. In a typical experiment, a certain amount of WSNR or SN (0.6–3.0 g L^{-1}) was dispersed into the reaction flask containing 100–500 mL of MB (10–100 mg L^{-1}) solution to initiate the reaction. The solution pH (3–10) was previously adjusted to the desired value by addition of dilute NaOH/HCl. At predetermined intervals, 10 mL aliquots were withdrawn and centrifuged, and the absorbance was measured by a UV–Vis spectrophotometer (Systronics 2201) at 660 nm (λ_{max}) to determine the residual MB concentration. Assuming sulphate as one of the decolorization products of MB, its concentration in the reactant solution at the end of the reaction was determined by ion chromatography (Metrohm) in conductance mode. The concentrations of Mn and Fe in the filtrate after the decolorization reaction of a few selected runs were also estimated by AAS to determine the amounts of Mn and Fe that get into the reactant solution through reductive dissolution. Since WSNR contains some finely divided carbon, it is expected that a small amount of MB may adsorb on the surface of WSNR. In order to roughly assess the amount of MB adsorbed, the whole amounts of WSNR added in several runs were separated by centrifugation, dispersed in 50 mL of distilled water of pH ~5.0 and stirred for a predetermined time of 1–3 h to desorb the adsorbed MB. The concentration of the desorbed MB was determined spectrophotometrically. The amounts of MB desorbed from WSNR were never more than 2–3% of the total MB decolorized. All the reactions were carried out at least in duplicate, and average values are reported.

The kinetics of oxidative decolorization by WSNR and SN were determined using the data of experimental runs with an initial MB concentration of 30 mg L^{-1}, WSNR or SN of 0.6 g L^{-1} and pH ~ 3.0. The rate constants were calculated from the plots of $\ln(C_t/C_0)$ versus time where C_0 and C_t represent the initial MB concentration and the concentration at time t, respectively.

3. Results and discussion

3.1. Characteristics of leached residue

The chemical analyses of SNR and WSNR along with SN are given in Table 1. It is evident that the SNR mainly contains Mn, Fe, Si and Al. Manganese(IV) remains the major constituent (~45% of total manganese) although a sizeable amount of Mn(IV) is reduced during the reduction-roast ammoniacal leaching. However, the Mn/Fe ratio of SNR

Table 1. Chemical compositions of manganese nodule (SN), and untreated (SNR) and water-washed (WSNR) manganese nodule leached residue (in wt.%).

Element/Oxide	SN	SNR	WSNR
Mn(T)*	25.0	25.66	25.85
Mn(II)	0.11	14.02	13.71
Mn(III)	1.02	4.87	4.92
Mn(IV)	23.87	6.77	7.22
Fe(T)	7.82	9.92	10.03
SiO_2	17.06	17.07	17.25
Al_2O_3	3.84	4.01	4.11
C	0.178	5.27	5.59
S	0.001	0.37	0.14
P	0.04	1.34	0.18
CaO	0.38	0.43	0.45
MgO	4.24	4.69	4.73
Co	0.083	0.035	0.039
Ni	0.94	0.079	0.071
Cu	0.86	0.26	0.135
Zn	0.18	0.12	0.13
Moisture	–	7.96	6.18
Loss of Ignition	18.31	15.95	17.50

*The values against Mn^{2+}, Mn^{3+} and Mn^{4+} represent respective wt.% out of total manganese content in the samples.

and WSNR is reduced to 2.8, compared with 3.19 for SN. On washing with distilled water, only a marginal change in weight percentages of Mn, Fe, SiO_2, C, CaO and MgO is observed, whereas there is a significant loss of adsorbed metal ions like Cu and Ni along with S and P. Hence, it is reasonable to believe that the S and P in SNR, generated by roasting of SN with fuel, are mostly present in the soluble forms. The loss on ignition of WSNR is ~2.5% higher than that observed with SNR.

Particle size analysis shows the SNR mainly consists of very fine particles with a mean particle diameter (d_{50}) of 17.8 μm. The BET surface areas of SN, SNR and WSNR are 130, 60.9 and 66.7 $m^2\ g^{-1}$, respectively. The decrease in surface area of SNR is presumably due to loss of porosity of SN and the formation of manganese carbonate and silicate when SN is roasted. On washing of SNR with water, the surface area is marginally increased because of an increased number of accessible pores. The average pore diameter, however, remains practically the same (~40 Å) in all three samples.

The pH_{pzc} of WSNR was found to be 6.5. Since WSNR is a complex material containing hydr(oxides) of Mn, Fe, Al and Si along with carbonate and silicate of Mn, the observed value of pH_{pzc} is intermediate of pH_{pzc} values reported for MnO_2/MnOOH (2.0–2.3), FeOOH (~7.5), Al_2O_3 (~8.1) and SiO_2 (~2.0) [28,31,32]. The observed value is also relatively higher than that reported for untreated sea nodule (4.5) [28]. This may be attributed to the lowering of the buffering capacity of metal (hydr)oxides in reduction-roasted leached reside due to their dehydration. The increase in pH_{pzc} with the increase in temperature of heat treatment has previously been reported for sea nodules [31].

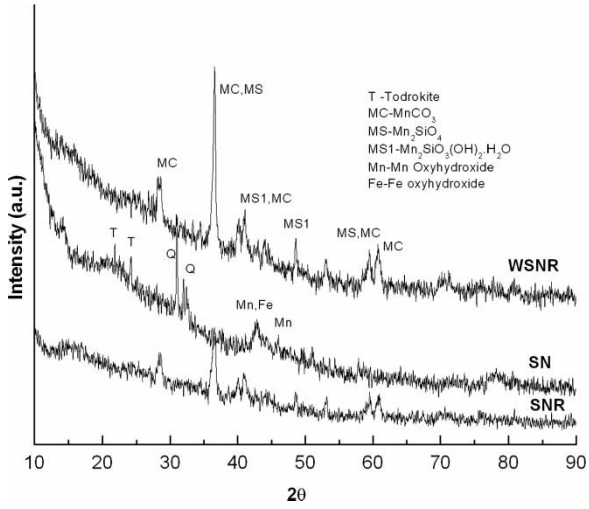

Figure 1. Powder X-ray diffraction of sea nodules (SN), leached residue (SNR) and washed leached residue (WSNR).

The XRD patterns of air-dried SN, SNR and WSNR are given in Figure 1. It is seen that SN is mostly amorphous in nature with a few low intensity peaks corresponding mainly to quartz todorokite, quartz and clay minerals such as phillipsite (File No. 02-0084), merlinolite (File No. 29-0989) and cryptomelane (File No. 34-168). No other peaks for either Mn or Fe hydr(oxide) are observed owing to their poor crystallinity or the amorphous nature of SN. After reduction roasting followed by leaching, the XRD peaks at 21.8° and 24.1°, due to todorokite, have completely disappeared. The characteristic peaks of quartz have also disappeared owing to its consumption in the formation of metal, especially Mn, silicates. This is evident from the appearance of new peaks in SNR for manganese silicates (indicated as MS, MS1 in Figure 1). In addition, the formation of $MnCO_3$ is also evident from the appearance of its characteristic peaks (denoted as MC, Figure 1) in SNR (File No. 44-1472). No change in the positions of characteristic XRD peaks is observed on washing of the SNR with distilled water.

The TG-DTA of SNR revealed (not shown) multi-stage weight losses in the ranges 25–310 °C (5%), 310–580 °C (10%) and >580 °C (2%) with two DTA peaks centred at 80 °C (endothermic) and 400 °C (exothermic). The first-stage weight loss (~5%) is attributed to the loosely bound water molecules, whereas the second- and third-stage losses are mainly attributed to the decomposition of metal carbonates as well as the elease of structural water from hydr(oxides) and clay minerals. The total weight loss (~17%) compares well with that obtained from the chemical analysis (loss of ignition, ~16%) and is about 11% less than the value obtained with leached residue generated by reductive ammoniacal leaching of SN without prior roasting using $NH_4OH/(NH_4)_2SO_4$ [28].

The FT-IR spectra of air-dried SN, SNR and WSNR are presented in Figure 2. The strong absorption bands

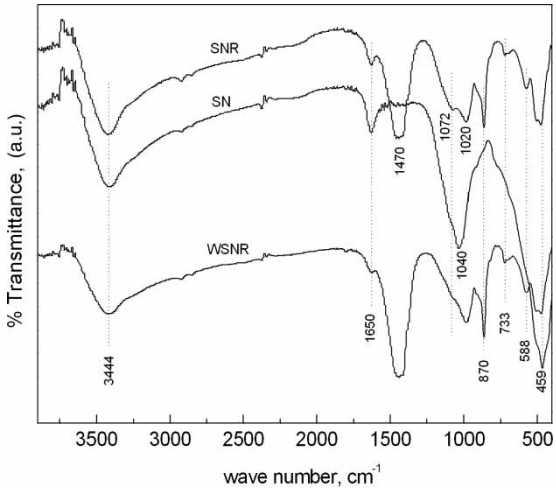

Figure 2. FT-IR spectra of sea nodules (SN), leached residue (SNR) and washed leached residue (WSNR).

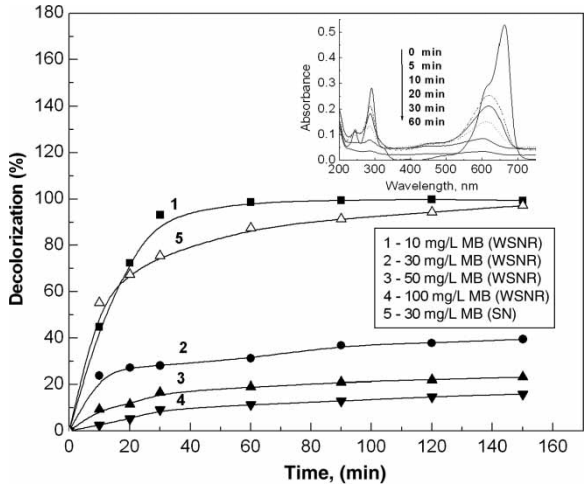

Figure 3. Time profile of MB decolorization at varying initial MB concentrations with washed leached residue (WSNR) and sea nodule (SN) at pH $\sim$ 3.0 and WSNR/SN $= 0.6\,\mathrm{g\,L^{-1}}$. Inset: UV–Vis spectral change of MB solution with time.

at $\sim$3445 $\mathrm{cm^{-1}}$ and $\sim$1650 $\mathrm{cm^{-1}}$ in all three samples are attributed to –OH stretching and bending modes of vibrations [33]. The band at 1040 $\mathrm{cm^{-1}}$ in SN corresponds to Si–O/Si–O–Al of silicate materials. The appearance of new absorption bands at 1470/1070 and 870 $\mathrm{cm^{-1}}$ for SNR are due to ν(C–O) and δ(OCO) of carbonate ion, respectively [33,34]. The occurrence of these bands in SNR provides further evidence in favour of the formation of $MnCO_3$ during the reduction-roasting process of SN with fuel. On washing of SNR with distilled water, the positions of the majority bands retain the same except for the disappearance of the band at 1072 $\mathrm{cm^{-1}}$ due to the loss of a small amount of loosely bound NH_3 or sulphate on washing [28]. The sulphate is generated from the impurities of the fuel during the reduction roasting of the sea nodule.

3.2. Decolorization of methylene blue

3.2.1. Effect of initial concentration of MB

The extent of MB decolorization by WSNR with time at varying initial MB concentrations (10–100 $\mathrm{mg\,L^{-1}}$) under identical conditions is shown in Figure 3 along with the decolorization activity of SN at a representative initial MB concentration. It is seen that the decolorization of MB is relatively fast at the beginning and decreases as the reaction progresses. At low concentration (10 $\mathrm{mg\,L^{-1}}$), MB is completely decolorized by WSNR (0.6 $\mathrm{g\,L^{-1}}$) within 1 h, which is also evident from the UV–Vis spectra of MB recorded with reaction time (Figure 3, inset). The initial peaks at 614 and 664 nm are merged into a relatively broad peak centred at $\sim$614 nm within 2 min of the reaction. Thereafter, the peak intensity is reduced progressively with a shift towards a lower wavelength until the reactant solution turns colourless. On the other hand, the intensities of MB bands at 292 and 245 nm are reduced progressively without any shift in their positions. A similar spectral change has been reported for catalytic oxidation of MB by β-MnO_2 nanorods [18].

The time profiles of MB decolorization show that the decolorization is substantially decreased with increase in initial MB concentration. For example, the extent of decolorization after 2.5 h decreases from 40% to 14% and from 93% to 10% with increase in concentration of MB from 30 to 100 $\mathrm{mg\,L^{-1}}$ for WSNR and SN, respectively. This decrease may be attributed to the formation of a surface precursor complex between WSNR/SN and MB at a rate-limiting step prior to electron transfer from MB to the active metal centre of WSNR/SN leading to MB decolorization. A similar trend has also been observed for MB decolorization by manganese nodule and other oxides [18,19]. Moreover, the previous studies on oxidative degradation of organic matters, including dyes, by Mn oxides/nodules have also reported the formation of a surface precursor complex followed by the release of oxidation products and Mn(II) arising from the reduction of Mn(IV,III) oxides. Based on the above it appears that the surface reactivity and the number of available sites are two critical factors which control the decolorization of MB. In the present case, the decrease in MB decolorization at higher concentration is a result of the saturation of active surface sites in WSNR/SN for further formation of a precursor complex followed by electron transfer. The higher activity of SN in comparison to WSNR is primarily due to the presence of a much higher percentage of the active component, mainly Mn(IV), in SN.

3.2.2. Effect of catalyst amount

The results of MB decolorization with varying amounts of WSNR (0.6 to 3.0 $\mathrm{g\,L^{-1}}$) indicate that the decolorization rate is fast at the beginning (up to $\sim$20 min) and then follows a slow decolorization process irrespective of the amount of WSNR. It is seen that the extent of MB decolorization decreases from 86.1% to 33.5% with the decrease

in WSNR amount from 3.0 to 0.6 g L^{-1}. This lowering of decolorization activity is mainly due to the overall decrease in the active surface area and the components of WSNR for complexation with MB leading to the products. It may also be noted that the role of iron (hydr)oxides in MB decolorization is practically negligible in the present case because of their lower reduction potential (0.655–0.757 V) compared with Mn(III,IV) (hydr)oxides (1.27–1.50 V) [19].

3.2.3. *Effect of initial pH of MB solution*

As the oxidative decolorization of MB appears to involve its diffusion on to the WSNR surface to form a surface precursor complex followed by electron transfer, the pH of the reaction medium is expected to play a crucial role. Furthermore, it is necessary to optimize the working pH for the practical application of WSNR as a catalyst for MB decolorization. As such the catalytic efficiency of WSNR/SN for MB decolorization in the pH range 3–10 was evaluated and the results obtained are presented in Figure 4. It is evident (Figure 4, inset) that SN showed better activity than WSNR over the whole pH range owing to a higher percentage of the active component, mainly Mn(IV), in SN. The progressive decrease in MB decolorization by WSNR with increase in pH up to 10 may be explained as follows.

At lower pH, the surface of WSNR is positively charged ($pH_{pzc} = 6.5$), which does not favour an electrostatic interaction with the cationic form of MB, thus leading to the formation of a surface complex. As the pH increases, the surface charge of WSNR becomes less positive and there is also a decrease in $N(CH_3)_2$ protonation in MB. Both these effects do not favour the formation of a surface complex between WSNR and MB. Hence, the other reason for the enhanced activity of WSNR at lower pH could be due to a favourable reduction potential of Mn(III,IV) hydr(oxide)/Mn(II) couple for electron transfer. A sharp increase in oxidizability of Mn(IV) oxide with an increase in H^+ ion concentration has also been reported in the degradation of F3B dye with natural manganese mineral [17]. On the other hand, the surface charge of WSNR becomes negative at pH > 6.5 ($pH_{pzc} = 6.5$), which favours the adsorption of Mn(II) formed by the reduction of Mn(III,IV) hydr(oxide) during MB decolorization. This in turn inhibits the adsorption of MB on the WSNR surface. Also it has been reported that there is a decrease in redox potential of Mn(III,IV) hydr(oxide)/Mn(II) couple at higher pH [19]. The combined effect of the above two factors results in a decrease in oxidative decolorization of MB by WSNR at higher pH [17,19].

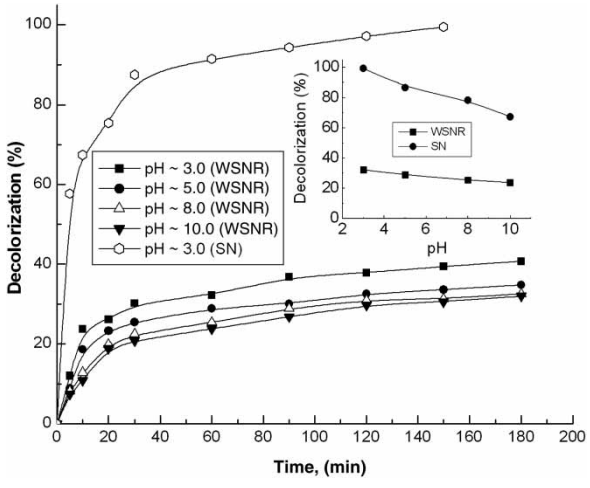

Figure 4. Time profile of MB decolorization at different pH with washed leached residue (WSNR) and sea nodule (SN) (WSNR/SN = 0.6 g L^{-1}, MB = 30 mg L^{-1}). Inset: pH effect on MB decolorization.

3.2.4. *Effect of hydrogen peroxide*

Hydrogen peroxide, alone or in conjunction with other materials, is used for oxidation and degradation/decolorization of many harmful organic compounds including dyes. The addition of a small amount of catalyst to a system containing H_2O_2 may lead to the generation of free radicals like $^{\bullet}OH$ with a reasonably high reduction potential (2.3 eV) that facilitates faster degradation of organic compounds [16]. Also it is well known that the presence of manganese-based minerals/materials significantly accelerates the decomposition of H_2O_2 [20,35], which may in turn enhance the oxidative decolorization. As such it is believed that the presence of H_2O_2 may further accelerate the activity of WSNR for oxidative decolorization of MB. In fact a significant enhancement in activity has been observed in the case of MB degradation by β-MnO_2 in the presence of H_2O_2 [18]. The variation of [H_2O_2] (Table 2) indicates that MB decolorization increases with increase in [H_2O_2] at least up to 0.15 M, beyond which the effect is marginal or remains the same. This trend is very similar to that observed for degradation/decolorization of dyes using polyaniline/MnO_2 in the presence of H_2O_2 [16]. As the reaction is carried in the presence of air, the increase in the percentage of MB decolorization is not due to the oxidation by oxygen released from H_2O_2 in the presence of WSNR. In fact, in a previous study on MB degradation by β-MnO_2 in the presence of H_2O_2, Zhang et al. [18] showed that the extent of degradation is practically unaffected even with

Table 2. Effect of H_2O_2 concentrations on MB decolorization using WSNR. Reaction conditions: MB, 30 mg L^{-1}; pH ~ 3.0; WSNR = 0.6 g L^{-1}; time; 180 min.

[H_2O_2], mol dm^{-3}	Decolorization, %
0.0	39.20
0.02	44.01
0.10	55.90
0.15	62.42
0.20	63.50

constant bubbling of O_2 into the reactant solution. Hence the free-radical species (like $HO^{\bullet}$, $HOO^{\bullet}$ or $O_2^{-\bullet}$), generated *in situ* from H_2O_2, is more likely to be responsible for the increase in oxidative decolorization of MB. The marginal effect of $[H_2O_2]$ beyond 0.15 M is presumably due to the well-known free-radical scavenging effect via the reaction of free radicals with excess H_2O_2 [36].

3.2.5. *Effect of added electrolyte*

As it is believed that the degradation/decolorization of dyes over manganese oxides/minerals proceeds through formation of specific surface complexes followed by electron transfer, the role of the added electrolyte is important. As such, MB decolorization was carried out in the presence of varying concentrations of NaCl (0.02–0.20 mol L^{-1}), and the results obtained are shown in Figure 5. The pH of the suspension at the end of the reaction in each run was measured and was found to be slightly higher than the pH initially adjusted. Although there is a progressive increase in the percentage of decolorization, the salt effect is more significant at lower concentration (0.02 mol L^{-1} NaCl) presumably because of the following two factors. In the presence of NaCl, there is a possible decrease in the thickness of the electrical double layer formed between WSNR and water [17]; as a consequence the dye molecule moves closer to the WSNR surface, which facilitates the formation of a surface complex. Also the solubility of the MB is believed to decrease upon addition of NaCl owing to the common ion effect, which favours the exclusion of dye molecules from the solution phase to the particle surface. The second factor for the increased percentage of MB decolorization may be the increase in the surface potential of the solid catalyst in the presence of added electrolyte. The rate enhancement of dye degradation in the presence of electrolyte has also been reported in an earlier study [17].

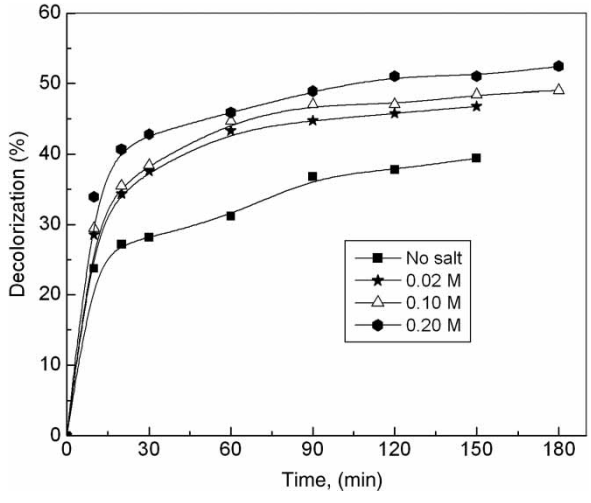

Figure 5. Effect of [NaCl] on MB decolorization at pH ~3.0, WSNR = 0.6 g L^{-1}, MB = 30 mg L^{-1}.

3.2.6. *Kinetics of methylene blue decolorization*

The time-course oxidative decolorization plots (Figures 3 and 4) clearly indicate that the decolorization process takes place in two steps. In typical runs with an initial MB concentration of 30 mg L^{-1}, pH ~ 3.0 and WSNR (0.6 g L^{-1}), the derived rate constants for first- and second-stage decolorization are found to be 2.4×10^{-2} and 1.0×10^{-3} min^{-1}, respectively, whereas relatively higher rate constants for the first (8.2×10^{-2} min^{-1}) and second (1.8×10^{-2} min^{-1}) steps are observed for SN under identical conditions. It may be noted that two-stage oxidative decolorization of MB with sea nodule (pelagite) as catalyst, with comparable rate constants, i.e. 1.4×10^{-2} min^{-1} (first stage) and 4.6×10^{-3} min^{-1} (second stage), has been reported previously [19]. Furthermore, the observed rate constants are also comparable with those reported for oxidative degradation of red F3B dye by natural manganese mineral, $(3.3–6.26) \times 10^{-2}$ min^{-1}, where surface chemical reaction was proposed as the rate-limiting step in the overall interface process [19]. In the present study, the decrease in the rate of MB decolorization in the later stage may be partly attributed to the increase in pH of the reaction medium and the adsorption of Mn(II) on the WSNR surface, which in turn reduce the extent of surface complexation with MB. The pHs of the reaction mixture at the end of the reaction are always found to be higher than the initial pH, owing to consumption of H^+ in the redox process. In comparison, the oxidative degradation of several organic pollutants by manganese oxide is found to follow pseudo-first-order kinetics with respect to organic pollutant concentration at the beginning but deviates at the later stage of the process On the other hand, the oxidative degradation of 2,4,6-trinitrotoluene (TNT) by birnesite (δ-MnO_2) was found to follow a pseudo-first-order kinetics with respect to birnesite loading for the entire period of the reaction [37].

3.2.7. *Release of Mn(II) and sulphate*

Oxidative decolorization of MB was further confirmed by estimating the Mn(II) and sulphate released at the end of the reaction in a few selected experiments.

It was observed that the solubility of manganese (Mn(II), Mn(III) and Mn(IV)) or iron (Fe(II) and Fe(III)) from WSNR in aqueous solution at pH ~3.0 without MB is very low ($\leq$3 mg L^{-1}) and remains almost unchanged with time. However, a part of the Mn(III,IV) of WSNR is expected to go into solution as Mn(II) during the oxidative decolorization of MB, and the amount of Mn release primarily depends on the experimental conditions. The release of Mn(II) at varying pHs and WSNR amounts are presented in Table 3. In fact, the values of Mn(II) content in solution are the net results from the reductive dissolution of Mn(III,IV) and surface adsorption of Mn(II) on Mn and Fe (hydr)oxides of WSNR. It is seen that the release of Mn(II) is significant at lower pH and decreases progressively with increase in

Table 3. Release of Mn(II) during oxidative decoloriazation of methylene blue using WSNR. Reaction conditions: MB, 30 mg L^{-1}; time, 180 min.

WSNR/SN dose (g L^{-1})	pH	Mn(II) released[a], mg L^{-1}
0.6	3.08	11.5
1.6	3.05	13.1
3.0	3.03	16.0
0.6	5.01	6.82
0.6	8.02	3.11
0.6	10.0	1.21
0.6	3.06	16.3[b]
0.6	3.06	12.5[c]

[a]Average of at least duplicate measurements.
[b]Under identical conditions but with $[H_2O_2] = 0.0.2$ M.
[c]For SN without H_2O_2.

pH. It is also observed that the release of Mn(II) in the case of SN, under identical conditions, is not higher than that obtained for WSNR, even though the former has much higher activity, which in turn reduces the higher amount of Mn(IV) of SN. This is most likely due to the relatively higher adsorption capacity of SN for Mn(II) in comparison to WSNR.

One of the major products of oxidative decolorization of MB is sulphate. The qualitative $BaCl_2$ test with the reactant solutions at the end of the reaction indicates the formation of sulphate during the oxidative decolorization of MB. In a typical experiment with an initial MB of 30 mg L^{-1}, WSNR of 0.6 g L^{-1} and pH ~3.0, the formation of sulphate is estimated to be 2.51 ± 0.05 mg L^{-1}, which is close to the expected value when 35% of MB is decolorized. Under identical conditions in the control (WSNR without MB), the release of sulphate from WSNR is ~0.051 mg L^{-1} (~2.1% of total sulphate released), indicating that the sulphate is mainly released from MB during its oxidative decolorization by WSNR. Interestingly the release of Fe(II) into the reactant solution, as the reduced product of Fe(III) hydr(oxide), is negligible, indicating that the contribution of Fe (hydr)oxides of WSNR towards oxidative decolorization of MB is insignificant. This is primarily due to much lower reduction potentials of Fe(III) (hydr)oxide minerals compared with Mn(III,IV) (hydr)oxide minerals [19].

4. Conclusions

The present study is an attempt to find an alternative use for the huge amounts of leached residue likely to be generated after selective reduction-roasting ammoniacal leaching of strategic metals from sea nodules. Physicochemical characterizations of sea-nodule residue indicate significant reduction of Mn(IV)/Fe(III) during the leaching process and the formation of $MnCO_3$. Although water-washed sea-nodule residue (WSNR) is found to be effective for decolorization of MB, the activity is relatively lower than that of the parent sea nodule. The extent of decolorization is dependent on several factors and is found to decrease with increase in pH values and initial MB concentration. The kinetic study shows a two-step consecutive decolorization process; the rate constant of the first step is ~10 times higher than that of the second step. The activity of WSNR is enhanced in the presence of H_2O_2 and NaCl at least at lower concentrations. Manganese(II) is found to release into solution from WSNR/SN during the decolorization process, which decreases with increase in pH values. The ion chromatographic study shows sulphate to be one of the major decolorization/degradation products of MB. The formation of a surface complex between WSNR and MB at a rate-limiting step, followed by electron transfer from MB to the active metal centre of WSNR and release of products, is most likely to be operative during the decolorization process.

References

[1] M.S. Lucas and J.A. Peres, *Decolorization of the azo dye Reactive Black 5 by Fenton and photo-Fenton oxidation*, Dyes Pigm. 71 (2006), pp. 236–244.
[2] Q. Zhuo, H. Ma, B. Wang, and F. Fan, *Degradation of methylene blue: Optimization of operating conditions through a statistical technique and environmental estimate of the treated water*, J. Hazard. Mater. 153 (2008), pp. 44–51.
[3] D.H. Bache, M.D. Hossain, S.H. Al-Ani, and P.J. Jackson, *Optimum coagulation conditions for a coloured water in terms of floc size, density and strength*, Water Supply 9 (1991), pp. 93–102.
[4] U. Bali, E. Catalkaya, and F. Sengul, *Photodegradation of Reactive Black 5, Direct Red 28 and Direct Yellow 12 using UV, UV/H_2O_2 and UV/H_2O_2/Fe^{2+}: A comparative study*, J. Hazard. Mater. 114 (2004), pp. 159–166.
[5] A. Bousher, X. Shen, and R. Edyvean, *Removal of coloured organic matter by adsorption onto low-cost waste materials*, Water Res. 31 (1997), pp. 2084–2092.
[6] K. Dutta, S. Mukhopadhyay, S. Bhattacharjee, and B. Chaudhuri, *Chemical oxidation of methylene blue using a Fenton-like reaction*, J. Hazard. Mater. 84 (2001), pp. 57–71.
[7] V.S.F. Leitao, M.E.A. de Carvalho, and E.P.S. Bon, *Lignin peroxidase efficiency for methylene blue decolonization: Comparison to reported methods*, Dyes Pigm. 74 (2007), 230–236.
[8] M, Panizza, A. Barbucci, R. Ricotti, and G. Cerisola, *Electrochemical degradation of methylene blue*, Sep. Purif. Technol. 54 (2007), pp. 382–387.
[9] N. Daneshvar, D. Salari, and A.R. Khataee, *Photocatalytic degradation of azo dye acid red 14 in water on ZnO as an alternative catalyst to TiO_2*, J. Photochem. Photobiol. A 162 (2004), pp. 317–322.
[10] W. Du, Y. Xu, and Y. Wang, *Photoinduced degradation of Orange II on different iron (hydr)oxides in aqueous suspension: Rate enhancement on addition of hydrogen peroxide, silver nitrate, and sodium fluoride*, Langmuir 24 (2008), pp. 175–181.
[11] J. Li, W. Ma, C. Chen, J. Zhao, H. Zhu, and X. Gao, *Photodegradation of dye pollutants on one-dimensional TiO_2 nanoparticles under UV and visible irradiation*, J. Mol. Catal. A 261 (2007), pp. 131–138.
[12] T. Matsunaga and M. Inagaki, *Carbon-coated anatase for oxidation of methylene blue and NO*, Appl. Catal. B 64 (2006), pp. 9–12.

[13] K.M. Parida, N. Sahu, N.R. Biswal, B. Naik, and A.C. Pradhan, *Preparation, characterization and photocatalytic activity of sulfate-modified titania for degradation of methyl orange under visible light*, J. Colloid Interface Sci. 318 (2008), pp. 231–237.

[14] J.Q. Chen, D. Wang, M.X. Zhu, and C.J. Gao, *Study on degradation of methyl orange using pelagite as photocatalyst*, J. Hazard. Mater. 138 (2006), pp. 182–186.

[15] J. Ge and J. Qu, *Degradation of azo dye acid red B on manganese dioxide in the absence and presence of ultrasonic irradiation*, J. Hazard. Mater. 100 (2003), pp. 197–207.

[16] R.G. Gemeay, I.A. El-Sharkawy, I.A. Mansour, and A.B. Zaki, *Catalytic activity of polyaniline/MnO_2 composites towards the oxidative decolorization of organic dyes*, Appl. Catal. B 80 (2008), pp. 106–115.

[17] R. Liu and H. Tang, *Oxidative decolorization of direct light red F3B dye at natural manganese mineral surface*, Water Res. 34 (2000), pp. 4029–4035.

[18] W. Zhang, Z. Yang, X. Wang, Y. Zhang, X. Wen, and S. Yang, *Large-scale synthesis of β-MnO_2 nanorods and their rapid and efficient catalytic oxidation of methylene blue dye*, Catal. Commun. 7 (2006), pp. 408–412.

[19] M.X. Zhu, Z. Wang, and L.Y. Zhou, *Oxidative decolourisation of methylene blue using pelagite*, J. Hazard. Mater. 150 (2008), pp. 37–45.

[20] K.M. Parida, P.K. Satapathy, and N.N. Das, *Studies on Indian Ocean manganese nodules. I. Physico-chemical characteristics and catalytic activity of ferromanganese nodules*, J. Colloid Interface Sci. 173 (1995), pp. 112–118.

[21] S. Acharya, M.K. Ghosh, S. Anand, and R.P. Das, *Leaching of metals from Indian Ocean nodules in SO_2–H_2O–H_2SO_4–$(NH_4)_2SO_4$ medium*, Hydrometallurgy 53 (1999), pp. 169–175.

[22] R.K. Jana, S. Srikanth, B.D. Pandey, V. Kumar, and Premchand, *Processing of deep sea manganese nodule at NML for recovery of copper, nickel and cobalt*, Met. Mater. Processes 11 (1999), pp. 133–139.

[23] R.K. Jana, B.D. Pandey, and Premchand, *Ammoniacal leaching of roast reduced deap-sea manganese nodules*, Hydrometallurgy 53 (1999), pp. 45–56.

[24] H. Li, Y. Feng, S. Lu, and Z. Du, *Bioleaching of valuable metals from marine nodule under anaerobic condition*, Miner. Eng. 18 (2005), pp. 1421–1422.

[25] Y. Wang, Z. Li, and H. Li, *A new process for leaching metal values from Ocean polymetallic nodules*, Miner. Eng. 18 (2005), pp. 1093–1098.

[26] K.M. Parida, S. Mallick, and S.S. Dash, *Studies on manganese nodule leached residues 2. Adsorption of aqueous phosphate on manganese nodule leached residues*, J. Colloid Interface Sci. 290 (2005), pp. 22–27.

[27] A. Agrawal, K.K. Sahu, and B.D. Pandey, *Kinetic and isotherm studies of cadmium adsorption on manganese nodule residue*, J. Hazard. Mater. 137 (2006), pp. 915–924.

[28] N.N. Das and R.K. Jana, *Adsorption of some bivalent heavy metal ions from aqueous solutions by manganese nodule leached residues*, J. Colloid Interface Sci. 293 (2006), pp. 253–262.

[29] F. Klose, P. Scholz, G. Kreisel, B. Ondruschka, R. Kneise, and U. Knopf, *Catalysts from waste materials*, Appl. Catal. B 28 (2000), pp. 209–221.

[30] C.P. Huang and F.G. Ostavic, *Removal of Cd(II) by activated carbon adsorption*, J. Environ. Eng. Div. 104 (1978), pp. 863–878.

[31] S. Maity, S. Chakravarty, S. Bhattacharjee, and B.C. Roy, *A study on arsenic adsorption on polymetallic sea nodule in aqueous medium*, Water Res. 39 (2005), pp. 2579–2590.

[32] K.M. Parida, P.K. Satapathy, and N.N. Das, *Studies on Indian Ocean manganese nodules IV. Adsorption of some bivalent heavy metal ions onto ferromanganese nodules*, J. Colloid Interface Sci. 181 (1996), pp. 456–462.

[33] K. Nakamato, *Infrared Spectra of Inorganic and Coordination Compounds, Part B*, 5th ed., Wiley, New York, 1997.

[34] E.M. Nour, S.M. Teleb, N.A. AL-Khsosy, and M.S. Refat, *A novel method for synthesis of metal carbonates. I. Synthesis and infrared spectrum of manganese carbonate $MnCO_3 \cdot H_2O$, formed by the reaction of urea with manganese(II) salts*, Synth. React. Inorg. Met.-Org. Chem. 27 (1997), pp. 505–508.

[35] R.C.C. Costa, M.F.F. Lelis, L.C.A. Oliveira, J.D. Fabris, J.D. Ardisson, R.R.V.A. Rios, C.N. Silva, and R.M. Lago, *Novel active heterogeneous Fenton system based on $Fe_{3-x}M_xO_4$ (Fe, Co, Mn, Ni): The role of M^{2+} species on the reactivity towards H_2O_2 reactions*, J. Hazard. Mater. 129 (2006), pp. 171–178.

[36] J. De. Laat and T.G. Le, *Effects of chloride ions on the iron(III)-catalyzed decomposition of hydrogen peroxide and on the efficiency of the Fenton-like oxidation process*, Appl. Catal. B 66 (2006), pp. 137–146.

[37] K-H. Kang, D-M. Lim, and H. Shin, *Oxidative-coupling reaction of TNT reduction products by manganese oxide*, Water Res. 40 (2006), pp. 903–910.